Disorder-induced Floquet Topological Insulators

Paraj Titum,[1] Netanel H. Lindner,[1,2] Mikael C. Rechtsman,[3] and Gil Refael[1]

[1]*Institute of Quantum Information and Matter, Dept. of Physics, Caltech, Pasadena, CA 91125*
[2]*Technion Israel Institute of Technology, Haifa 32000, Israel*
[3]*Department of Physics, Technion - Israel Institute of Technology, Haifa 32000, Israel*

(Dated: March 5, 2014)

We investigate the possibility of realizing a disorder-induced topological Floquet spectrum in two-dimensional periodically-driven systems. Such a state would be a dynamical realization of the topological Anderson insulator. We establish that a disorder-induced trivial-to-topological transition indeed occurs, and characterize it by computing the disorder averaged Bott index, suitably defined for the time-dependent system. The presence of edge states in the topological state is confirmed by exact numerical time-evolution of wavepackets on the edge of the system. We consider the optimal driving regime for experimentally observing the Floquet-Anderson topological insulator, and discuss its possible realization in photonic lattices.

PACS numbers: 81.05.ue, 03.65.Vf, 73.43.Nq, 71.23.An

Topological states have been an ongoing fascination in condensed matter and recently led to the prediction [1–3] and realization [4–6] of various topological phases, and in particular topological insulators (TIs). TIs possess extraordinary properties (gapless edge states [7, 8], topological excitations [9]) and are expected to have myriad applications from spintronics to topological quantum computation [10]. Therefore, the quest to realize topological states has been in full thrust. One method proposes to dynamically induce topological phases by periodically driving a topologically trivial system out of equilibrium. These so-called Floquet topological insulators (FTI), for instance, might be obtained by irradiating trivial semiconductors with spin-orbit interaction [11, 12], or graphene-like systems, [13, 14]. Topological phases obtained by non-equilibrium processes introduce new means of controlling the phase, such as the frequency and the intensity of the drive. Also, while FTIs have gapless edge states as do topological insulators, with multiple resonances, they exhibit phases with no analog in equilibrium systems [15]. Remarkably, FTIs were recently experimentally realized in artificial photonic lattices where edge transport was observed [16], as well as in solid state systems [17]. The tunability of photonic systems is conducive to exploring a variety of topological effects. In particular, photonic experiments can realize tunable potentials even with prescribed disorder.

We are interested in the special interplay of disorder effects and topological behavior. In two dimensions, it has been shown [18] that ballistic edge modes are robust to disorder as long as there is a bulk mobility gap in the system. One can, therefore, measure quantized edge conductance even if the system is highly disordered. In contrast, disorder completely localizes the states of trivial non-interacting (spinless) 2-D systems. In the presence of a strong spin-orbit coupling, however, disorder can induce a topological phase transition from a trivial system into a topological Anderson insulator (TAI) phase, which exhibits quantized conductance at finite disorder strengths. TAIs were theoretically predicted in several electronic models [19–22], but to date have not been observed experimentally.

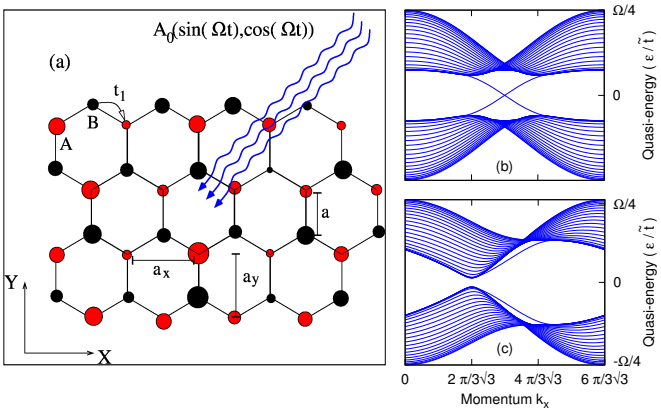

FIG. 1: (a) Schematic representation of the system indicating uniformly disordered graphene in the presence of a staggered mass potential and a circularly polarized light. Red-Black coloring indicates the staggered mass in the sublattices A and B, and the variable radius the disorder potential. (b) The Floquet band structure for the pure system with parameters, $A_0 = 1.43$, $M = 0$, and $\Omega/\tilde{t} = 12$. The system is topological and supports edge states. The bulk gap is given by the topological mass $\Delta/\tilde{t} \approx 0.75$. (c) A trivial Floquet band structure. All parameters are the same as (b) except $M/\tilde{t} = 0.85$.

Can disorder induce topological phases in trivial periodically-driven systems? Naively, we would think that disorder would destroy the conditions that give rise to Floquet topological phases. Nevertheless, we do find concrete examples where disorder induces a topological phase. Here we investigate such transitions in strongly driven systems, and describe their unique properties. The specific model we consider is a graphene-like lattice subject to circularly polarized light, with a staggered potential and on-site disorder. We obtain the phase diagram as a function of disorder strength by calculating the disorder-averaged bulk topological invariant viz., the Bott index. The time-evolution of wavepackets reveals the presence of gapless edge modes in the topologically non-trivial phase. As we explain below, the model we analyze is especially appealing as it is amenable to

experimental realization in photonic lattices.

Our starting point is the tight binding Hamiltonian of a honeycomb lattice subject to circularly polarized light,

$$H_0(t) = \sum_{<i\alpha,j\alpha'>} t_1 e^{iA_{ij}} c^\dagger_{i\alpha} c_{j\alpha'} + M\sigma^z_{\alpha\alpha'} c^\dagger_{i\alpha} c_{i\alpha'}, \quad \text{(1a)}$$

$$H(t) = H_0(t) + U_{\text{dis}} \quad \text{(1b)}$$

where $\alpha \in \{1,2\}$ indicates sublattices A and B, $A_{ij} = \frac{e}{\hbar}\mathbf{A}(t)\cdot(\mathbf{r}_i - \mathbf{r}_j)$ and $\vec{A} = A_0(\sin(\Omega t), \cos(\Omega t))$ is the vector potential for the incident circularly polarized light of frequency Ω. We consider only nearest neighbour hopping with magnitude t_1. σ^z is the Pauli matrix, and M is the staggered sublattice potential. $H_0(t)$ represents the clean limit for the system and $H(t)$ is the full Hamiltonian with U_{dis} the disorder potential. The disorder is chosen as an on-site chemical potential, and is diagonal in the real-space representation. We choose the natural system of units $\hbar = e = c = 1$ and set lattice spacing $a = 1$. The band width of the time-independent part of $H_0(t)$ is defined as W. Note that the model of Eq. (1) directly maps to the photonic lattice realization considered by Rechtsman et al. [16] (with M=0 and without disorder). In that model, the gauge field, $\mathbf{A}$, results from a fictional circularly-polarized electric field, which itself arises from the helicity of coupled optical waveguides. A nonzero mass, M, can be straightforwardly realized in the optical context by engineering the refractive indices of the waveguides to be different on the two sublattices, A and B. The disorder term in Eq. 1(b) can be realized by a randomization of refractive indices throughout the waveguide lattice.

The basic idea behind our consruction of a Floquet-Anderson topological phase is rather simple. A honeycomb lattice with a staggered potential , Eq. (1), has a gap M in both Dirac cones. A periodic drive alone also produces a gap, masses with opposite sign in the two Dirac cones. By second-order perturbation theory, this gap is simply $\tau_z A_0^2 v_F^2/\Omega$, where $\tau_z = \pm 1$ for the K and K' points. Thus, the drive induces effectively a Haldane model [23], and yields one of the first examples for a Floquet topological phase [13, 14]. Together, for weak and high-frequency ($\Omega \gg t_1$) drives, where perturbation theory is valid, the drive and the staggering compete, and the honeycomb model is reduced to the following continuum static Hamiltonian near the Dirac points:

$$H_{\text{eff}} = v_F(k_x\sigma_x\tau_z + k_y\sigma_y) + M\sigma_z + \frac{v_F^2 A_0^2}{\Omega}\sigma_z\tau_z. \quad \text{(2)}$$

In this limit, the system is topological when $M < v_F^2 A_0^2/\Omega$, with a Chern number $|C| = 1$, and trivial otherwise. The key is the effect of disorder: it effectively reduces the effect of the drive, but even more strongly it suppresses the staggering effect. If our drive is weaker than the effect of the staggered potential, $M > v_F^2 A_0^2/\Omega$, an increase in disorder may reverse the balance, and induce a topological phase (for a static analog, see Ref. [13]). In the supplementary material, we provide a Born-approximation disorder-averaging analysis of the disorder effects on the two competing gaps in the static limit [24].

The explanation above, however, relies on weak, high frequency drive, which in effect only produces a static perturbation. It does not capture the important situation in which the topological properties of the time dependent system are a result of a resonance connecting states of the original bulk band structure. In addition, we find that it is necessary to consider strong driving in order to observe the disorder induced topological phase. Below, we will establish the existence of the Floquet-Anderson topological phase beyond the limit of a weak, high frequency drive by considering both strong periodic drives, and frequencies that are sufficiently low that they induce resonances within the band of the static model, $\Omega < W$. To analyze the disorder-induced driven phases, we will calculate the topological invariant of the bulk bands numerically, as well as study the time-evolution of a wave packet on the edge.

Before plunging into the analysis, let us transform the problem defined in Eq. (1) into a time independent Hamiltonian. We define H^F as follows:

$$H^F_{nm} = n\Omega\delta_{nm} + \int_0^{2\pi/\Omega} dt e^{i\Omega(n-m)t} H(t) \quad \text{(3)}$$

The 'Floquet' indices n (and m) refer to replicas of the Hilbert space [24]. The eigenstates of H^F are the quasi-energies (ϵ), which are unique modulo the driving fequency, Ω, and are periodic in an quasi-energy "Brillouin" zone with period Ω. We set the boundaries of the quasi-energy zone at $\pm\Omega/2$. The off diagonal terms (in Floquet indices) of H^F_{nm} emerge from the hopping term in Eq. (1), $(H_0)_{ij} = t_1 \exp(iA_0\cos(\Omega t + \phi_{ij}))$, where (i,j) indicates hopping from site i to j and $\phi_{ij} = \pm\frac{\pi}{3}$ or 0. Therefore, $\left(H^F_{m,m+n}\right)_{ij} = t_1 i^n J_n(A_0)\exp(i\phi_{ij})$, where $J_n(A_0)$ are the Bessel functions of the first kind. For the range of parameters we consider, to efficiently use exact-diagonalization, we neglect $H^F_{m,m+n} = 0$ for $n \geq 2$. In this method, we will also truncate the $(H_F)_{nm}$ such that the Floquet indices obey $|n|, |m| \leq n_{max}$, with n_{max} determined through convergence tests. The typical quasi-energy spectrum of our model is given in Figs. 1 (b) and (c), where we have defined a renormalized hopping variable, $\tilde{t} = t_1 J_0(A_0)$.

The quasi-energy bandstructure encodes the topological properties of time-periodic Hamiltonians. While non-interacting equilibrium 2D Hamiltonians with broken time reversal symmetry are classified by the Chern number, periodically-driven systems require a more general topological invariant - the winding number - which counts the number of edge states at a particular quasi-energy [15]. In time independent systems without translational symmetry, the disorder-averaged Chern number can be calculated by averaging the Bott index, as defined by Hastings and Loring [25]. For our periodically-driven model, the disorder averaged winding number can be calculated using the Bott indices obtained from the eignevalues and eigenvectors of H_F, defined in Eq. (3) , and truncated to describe a finite number of replicas (for full details, see [24]). The Bott index at a particular quasi-energy,

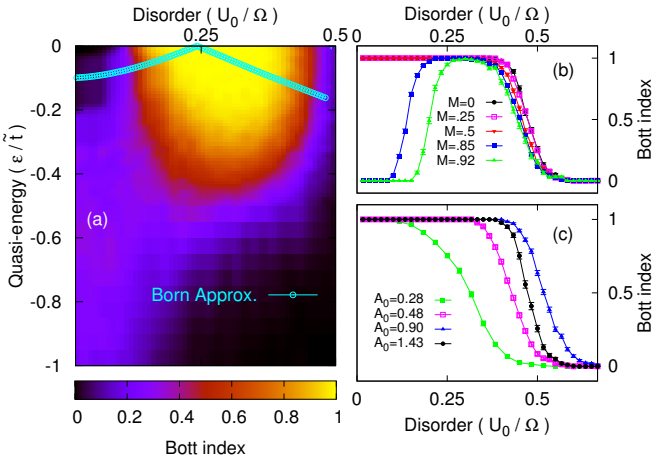

FIG. 2: (a) The Bott index (in color), as a function of the quasi-energy and the disorder strength. Edge states can be measured in the region where the Bott index, $C_b(0) = 1$. The quasi-energy gap is obtained within the Born approximation (cyan), as a function of disorder. The parameters for the system are $A_0 = 1.43$, $M/\tilde{t} = 0.85$ and system size is $(L_x, L_y) = (30, 30)$ (b) The Bott index as a function of disorder as we vary the staggered potential $M/\tilde{t} = 0,\ 0.5,\ 0.85,\ 1$ at quasi-energy $\epsilon = 0$ keeping t_1 and A_0 same as (a). (c) The Bott index as a function of disorder for different driving strengths, A_0, keeping fixed t_1 and $M/t_1 = 0$. We consider four cases: $A_0 = 0.28,\ 0.48,\ 0.90$ and 1.43. In all the parts we have set $\Omega/t_1 = 12J_0(1.43)$.

$C_b(\epsilon)$, for the truncated H_F, is the number of edge states at that quasi-energy [15]. Also, the Chern number of a quasi-energy band is simply the difference in the Bott indices at the band edges.

Let us first consider the case of $\Omega > W$ with no resonances. The parameters are chosen such that with no disorder the honeycomb lattice forms a trivial insulator, with its quasi-energy spectrum shown in Fig. 1 (c). The disorder averaged Bott index, C_b, as a function of disorder strength, U_0, and quasi-energy is shown in Fig. 2 (a). At very small disorder strengths, we notice that the index, $C_b(\epsilon = 0) = 0$ in the quasi-energy gap, and it is not quantized at other quasi-energies. Therefore, the phase is trivial. A topological phase emerges as disorder increases, and is manifested by the Bott index increasing to one, $C_b(0) \sim 1$. As expected, varying M while keeping the drive strength fixed, shifts the position of the trivial-topological transition (see Fig. 2 (b)). A qualitative description of this transition is provided by the disorder-averaged Born approximation given in the Supp. Mat. [24]; the analysis using this approximation, however, is clearly lacking quantitatively. The Bott index calculation reveals a topological phase induced by both disorder and drive, and, therefore, we identify it as a Floquet-Anderson topological insulator (FATI).

At disorder strengths that are considerably larger than the transition point, the FATI phase is destroyed and the system becomes fully localized at all quasi-energies. This transition is insensitive, by and large, to the staggered potential strength, as is evident from Fig. 2 (b); however, it does depend on the strength of driving, as shown in Fig. 2 (c). In order to observe the trivial to topological transition by increasing the disorder strength, it must occur well before the localization transition. This requires one to consider the effects of strong driving (where $A_0 \sim 1$). As discussed in the supplementary material, the finite size dependence of the Bott index as a function of quasienergy in the topological phase is in agreement with the presence of an extended state in the bulk quasi-energy band. The topological phase is protected to disorder as long as there is a 'mobility gap' in the quasi-energy spectrum, and some of its states are delocalized.

Next we examine the existence of edge states as a diagnostic for topological phases using a numerically exact time-evolution. The time-evolution operator for $H(t)$ is obtained in discrete time steps, δt, using a split-operator decompositon. The underlying honeycomb lattice [Fig. 1 (a)] is considered in a cylindrical geometry, where the boundary conditions are periodic along X and open along Y (see Fig. 3 (a). Initializing with a δ-function wavepacket at $\mathbf{r}_0 \equiv (x_0, y_0)$, the Green function, $G(\mathbf{r}, \mathbf{r}_0, t)$, is obtained from the time evolution operator, $U(t, 0)$. An evolution for N time periods ($T = 2\pi/\Omega$) yields $G_N(\mathbf{r}, \mathbf{r}_0, NT) = \langle \mathbf{r}|U(t = NT, 0)|\mathbf{r}_0\rangle$. The initial position, $\mathbf{r}_0$, is chosen properly to probe edge or bulk properties of the system. Compared to the analysis by exact-diagonalization of the Floquet Hamiltonian, in this method we do not need any approximations, and larger system sizes are accessible.

The propagator, $G_N(\mathbf{r}, \mathbf{r}_0, NT)$ is exactly the Floquet Green's function obtained from H^F [24]. So, information about the quasi-energy spectrum and eigenstates is obtained from the Fourier transform in time of the Green function, $G_N(\mathbf{r}, \mathbf{r}_0, \epsilon)$. For a disordered system, we calculate,

$$g_N(\mathbf{r}, \mathbf{r}_0, \epsilon) = \langle |G_N(\mathbf{r}, \mathbf{r}_0, \epsilon)|^2 \rangle, \tag{4}$$

where $\langle . \rangle$ indicates disorder averaging. The extended or localized nature of the states at quasi-energy ϵ is given by the spread of g_N defined as $\lambda_x(N)$, and $\lambda_y(N)$, along X and Y directions respectively.

We carry out the the time-evolution for a system with $A_0 = 1.434$, $M/\tilde{t} = 0.85$, at disorder strength $U_0/\tilde{t} = 3.5$, and $\Omega/\tilde{t} = 12$. The system has $(N_x \times N_y) \equiv (100 \times 30)$ points for each sublattice. These parameters correspond to the FATI phase and, therefore, we expect ballistic edge states at $\epsilon = 0$. The initial wavepackets are chosen in the A sublattice, on the two edges (cases (I) and (III)), and the bulk (II), as shown in Fig. 3 (a). After evolution for N time-periods, $g_N(\mathbf{r}, \mathbf{r}_0, 0)$, for all three cases is shown in Fig. 3 (c). For cases (I) and (III), g, is extended along X and localized in Y, indicating the presence of an edge state. The decay of g_N along X after some finite distance is due to finite time-evolution. The chiral nature of the edge states are also revealed by the direction in which $g_N(\mathbf{r}, \mathbf{r}_0, \epsilon)$ evolves as a function of N. Fig(3)(b) shows that $\lambda_x(N)$ increases linearly with total time of evolution, N, indicating that the edge states are ballistic and there is no backscattering from impurities. In contrast, bulk states are diffusive in nature till it spreads to the bulk localization

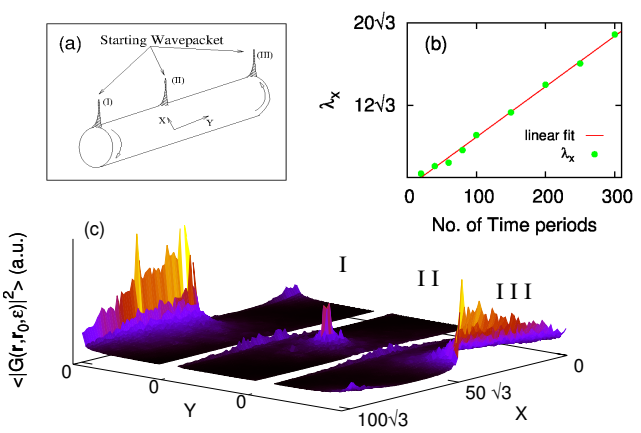

FIG. 3: (a) The cylindrical geometry for the time evolution of a starting δ-function wavepacket. Cases (I), (II) and (III) have the starting positions, $\mathbf{r}_0 \equiv (x_0, y_0)$ in the A sublattice at the left edge, bulk and right edge with $y_0/a_y = 0$, $N_y/2 - 1$ and N_y respectively. In all the cases, we fix $x_0/a_x = N_x/2$. (b) The spread of $g_N(\mathbf{r}, \mathbf{r}_0, 0)$ as a function of total time of evolution $T_f = NT$ along the X direction, for $\mathbf{r}_0$ corresponding to case (I). $\lambda_x(N)$ grows linearly, with a velocity $v_{\rm edge} = (0.09 \pm 0.001)a/T$. (c) $g_N = \langle |G_N(\mathbf{r}, \mathbf{r}_0, \epsilon = 0)|^2 \rangle$ in real space as a function of $\mathbf{r}$, for the three cases. We have set $N = 300$. In all the figures, each sublattice has $N_x \times N_y = 100 \times 30$ points and, g_N has been averaged over 400 realizations of disorder. The parameters for the system are $A_0 = 1.43$, and $M/\tilde{t} = 0.85$.

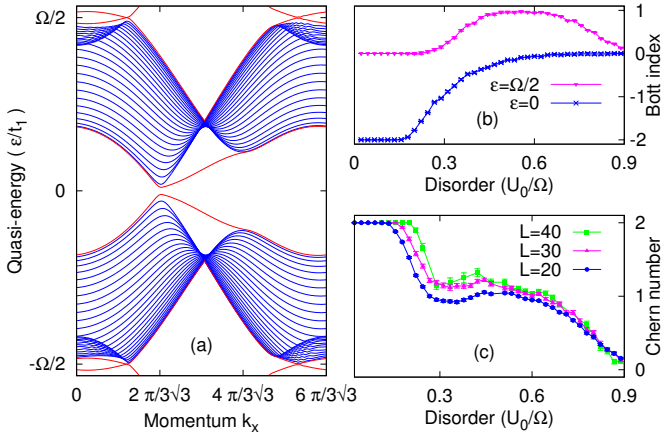

FIG. 4: (a) Bandstructure for the system for the case of a single resonance. Edge-states (shown in red) are observed at the two bulk band gaps at quasienergies $\epsilon/t_1 = 0$ and $\Omega/2$. The edge state do not cross the gap at $\epsilon = 0$ due to a staggered mass The parameters for the system are $A_0 = 0.75$, $M/t_1 = 0.3$, and $\Omega/t_1 = 9/2$. (b) The Bott index at a particular quasi-energy gap, $C_b(0)$ (blue) and $C_b(\Omega/2)$ (magenta), for the truncated Floquet Hamiltonian H_F. We have kept 9 Floquet bands. System size is $(L_x, L_y) = (30, 30)$ and they have been averaged over 300 disorder realizations. (c) Disorder averaged Chern number, $C_F = C_b(0) - C_b(\Omega/2)$, of a single Floquet band between $\epsilon = -\Omega/2$ and $\epsilon = 0$.

length. In our simulations we observe a finite amplitude on the edge when we start evolving a bulk wave packet. This is because the bulk localization length is larger than the width of the systems considered and, therefore, there is a finite overlap of the edge wavefunction with the bulk wavepacket. Therefore, we have shown the presence of gapless edge states protected against backscattering. This confirms the realization of a dynamical disorder-induced topological phase in a system that was trivial and gapped without disorder.

The FATI phase persists even when the drive frequency is $\Omega < W$, and a resonance occurs within the band structure. This case, a (presumably indirect) transition occurs between an FTI phase and the disorder-induced FATI phase. Furthermore, the FATI phase in this case can not be understood using the perturbative arguments behind Eq. (2) at all since the resonance alters the topological nature of all the Floquet bands in the problem [24]. Fig. 4 (a) shows the quasi-energy spectrum of the system at zero disorder. The gap at the resonance, $\epsilon = \Omega/2$ is topological with $|C_b(\Omega/2)| = 2$ and, thus, supports two edge states. The gap at the Dirac points is trivial, $|C_b(0)| = 0$, since the staggered mass M still dominates over the effect of the drive near $\epsilon = 0$. In Fig. 4 (b), we see that as disorder is increased, two transitions occur. A topological-to-trivial transition removes the edge states in the gap at the resonance ($\epsilon = \pm\Omega/2$). Another transition induces topological edge states at $\epsilon = 0$. From the finite system sizes investigated, it seems that the topological to trivial transition at $\epsilon = \Omega/2$ happens first and is unrelated to the transition at $\epsilon = 0$. Finally disorder becomes strong enough to localize the entire band, as in the high-frequency case discussed above. The Chern number of the band between these two quasi-energies, $C_F = C_b(0) - C_b(\Omega/2)$ changes from $|C_F| = 2$ to $|C_F| = 1$, and then to $|C_F| = 0$ (Fig. 4 (c)). The intermediate regime, with $|C_F| = 1$, is again identified as a FATI - it is a topological state that requires both disorder and a periodic drive to exist. The fact that this phase exists even in a system which is non-perturbatively affected by the periodic drive indicates the universality and robustness of the FATI phase.

This FATI phase is directly amenable to experimental observation. Recently, a photonic implementation of a topological insulator was experimentally demonstrated [16] in a structure composed of an array of evanescently coupled waveguides (a "photonic lattice"). In that system, the diffraction of light through the lattice is governed by the paraxial Schrödinger equation, wherein the spatial coordinate along the waveguide axis acts as the time coordinate. Specifically, the guided modes of the waveguides are analogous to atomic orbitals, and thus, the diffraction is governed by a tight-binding model. By fabricating the waveguides in a helical fashion, z-reversal symmetry is broken, resulting in a photonic Floquet topological insulator [11], with topologically-protected edge states.

The same photonic system may realize the FATI phase proposed above. The parameters needed to be controlled are the gauge field, A_0, the sublattice potential, M, and the degree of on-diagonal disorder, U_0. The strength of the gauge field in the photonic system is determined by the helix radius and period of the waveguides. The sublattice potential may be implemented by fabricating waveguides of different refractive

indices on the two different sublattices, which is straightforwardly done in the laser-writing fabrication process [26]. Diagonal disorder may be implemented by randomly varying the refractive indices of the waveguides in a similar fashion. The topological transition may then be probed by measuring the transmission through the photonic lattice for samples with different disorder strengths. For small disorder (when the system is topologically trivial), the presence of a bulk band gap (and no conducting edge states) will give rise to zero transmission through the sample. For disorder strengths above the transition, edge states will be present in the band gap and these will allow conduction through the sample: a direct experimental observable. Therefore, the Floquet topological Anderson insulator system may be implemented using an optical wavefunction in a photonic crystal structure, as opposed to an electronic wavefunction in a condensed matter system.

In summary, we have established the existence of a disorder induced Floquet Topological Insulator phase. Starting from a clean system that is trivial even in the presence of time-periodic driving, disorder renormalizes the parameters of the Hamiltonian in such a way as to make they system topological. Experimentally the parameters are in a range that can be achieved in a photonic lattice, and this could be a first experimental realization of the Topological Anderson Insulators.

We thank Kun W. Kim, Shu-Ping Lee, Victor Chua and S. M. Bhattacharjee for illuminating discussions. This work was funded by the Packard Foundation, and by the Institute for Quantum Information and Matter, an NSF Physics Frontiers Center with support of the Gordon and Betty Moore Foundation. NL acknowledges financial support by the Bi-National Science Foundation, and by ICore: the Israeli Excellence Center "Circle of Light".

[1] B. A. Bernevig, T. L. Hughes, and S.-C. Zhang, Science **314**, 1757 (2006).
[2] C. L. Kane and E. J. Mele, Phys. Rev. Lett. **95**, 146802 (2005).
[3] L. Fu, C. L. Kane, and E. J. Mele, Phys. Rev. Lett. **98**, 106803 (2007).
[4] M. König, S. Wiedmann, C. Brne, A. Roth, H. Buhmann, L. W. Molenkamp, X.-L. Qi, and S.-C. Zhang, Science **318**, 766 (2007).
[5] D. Hsieh, D. Qian, L. Wray, Y. Xia, Y. S. Hor, R. J. Cava, and M. Z. Hasan, Nature **452**, 970 (2008), ISSN 0028-0836.
[6] A. Roth, C. Brne, H. Buhmann, L. W. Molenkamp, J. Maciejko, X.-L. Qi, and S.-C. Zhang, Science **325**, 294 (2009).
[7] M. König, H. Buhmann, L. W. Molenkamp, T. Hughes, C.-X. Liu, X.-L. Qi, and S.-C. Zhang, Journal of the Physical Society of Japan **77**, 031007 (2008).
[8] B. Zhou, H.-Z. Lu, R.-L. Chu, S.-Q. Shen, and Q. Niu, Phys. Rev. Lett. **101**, 246807 (2008).
[9] X.-L. Qi, T. L. Hughes, and S.-C. Zhang, Nat Phys **4**, 273 (2008), ISSN 1745-2473.
[10] C. Nayak, S. H. Simon, A. Stern, M. Freedman, and S. Das Sarma, Rev. Mod. Phys. **80**, 1083 (2008).
[11] N. H. Lindner, G. Refael, and V. Galitski, Nat Phys **7**, 490 (2011), ISSN 1745-2473.
[12] N. H. Lindner, D. L. Bergman, G. Refael, and V. Galitski, Phys. Rev. B **87**, 235131 (2013).
[13] T. Kitagawa, T. Oka, A. Brataas, L. Fu, and E. Demler, Phys. Rev. B **84**, 235108 (2011).
[14] T. Oka and H. Aoki, Phys. Rev. B **79**, 081406 (2009).
[15] M. S. Rudner, N. H. Lindner, E. Berg, and M. Levin, Phys. Rev. X **3**, 031005 (2013).
[16] M. C. Rechtsman, J. M. Zeuner, Y. Plotnik, Y. Lumer, D. Podolsky, F. Dreisow, S. Nolte, M. Segev, and A. Szameit, Nature **496**, 196 (2013), ISSN 0028-0836, letter.
[17] Y. H. Wang, H. Steinberg, P. Jarillo-Herrero, and N. Gedik, Science **342**, 453 (2013).
[18] M. Onoda, Y. Avishai, and N. Nagaosa, Phys. Rev. Lett. **98**, 076802 (2007).
[19] J. Li, R.-L. Chu, J. K. Jain, and S.-Q. Shen, Phys. Rev. Lett. **102**, 136806 (2009).
[20] C. W. Groth, M. Wimmer, A. R. Akhmerov, J. Tworzydło, and C. W. J. Beenakker, Phys. Rev. Lett. **103**, 196805 (2009).
[21] Y. Xing, L. Zhang, and J. Wang, Phys. Rev. B **84**, 035110 (2011).
[22] J. Song, H. Liu, H. Jiang, Q.-f. Sun, and X. C. Xie, Phys. Rev. B **85**, 195125 (2012).
[23] F. D. M. Haldane, Phys. Rev. Lett. **61**, 2015 (1988).
[24] See supplementary material for details.
[25] T. A. Loring and M. B. Hastings, EPL (Europhysics Letters) **92**, 67004 (2010).
[26] A. Szameit and S. Nolte, Journal of Physics B: Atomic, Molecular and Optical Physics **43**, 163001 (2010).
[27] D. F. Martinez, Journal of Physics A: Mathematical and General **36**, 9827 (2003).
[28] N. H. Shon and T. Ando, Journal of the Physical Society of Japan **67**, 2421 (1998).

SUPPLEMENTARY MATERIALS

FLOQUET-BLOCH THEORY: DEFINITIONS

Let us start with the Hamiltonian $H(t)$ that is periodic in time,

$$\begin{aligned} H(\mathbf{k},t) &= H_0(\mathbf{k}) + V(t), \\ H(\mathbf{k},t) &= H(\mathbf{k},t+T), \text{ with } T = 2\pi/\Omega, \end{aligned} \tag{5}$$

as the time-period, Ω being the frequency. Here, H_0 contains the time-independent terms of the Hamiltonian. The states are given by the solution to the full time-dependent Schrödinger equation,

$$i\hbar\frac{\partial}{\partial t}\psi(\mathbf{k},t) = H(t)\psi(\mathbf{k},t) \tag{6}$$

The Floquet-Bloch theorem states that, the time-evolution operator can be written as

$$U(t,0) = \exp\left(-iH^F t\right) W(t), \text{ with } W(t+T) = W(t), \tag{7}$$

and H^F is a time-independent Hermitian operator. The form of Eq. (7) allows us to identify H^F as an effective time-independent Floquet Hamiltonian.

In order to define H^F, for the case at hand, the Fourier decomposition of the solution to Eq. (6) is used,

$$\psi(\mathbf{k},t) = \sum_n \psi_n(\mathbf{k}) e^{in\Omega t}, \tag{8}$$

$$= \sum_n \langle n|\psi^F\rangle\langle t|n\rangle, \text{ with } \langle t|n\rangle = e^{in\Omega t}. \tag{9}$$

In Eq. (9), we have introduced an additional register particle, $\{|n\rangle\}$, where $n \in \mathbb{Z}$. The Floquet Hamiltonian, H^F, is defined in a way such that $|\psi^F\rangle$ are eigenstates. Necessarily, it is defined in an extended Hilbert space $\mathscr{H} \otimes \{|n\rangle\}$, where $\mathscr{H}$ is the original Hilbert space of the Hamiltonian (see Eq. (6)). The time-dependent Schrödinger equation is rewritten in an effective time-independent form,

$$H^F|\psi^F\rangle = \epsilon|\psi^F\rangle, \tag{10}$$

where H^F is infinite dimensional. The eigenvalues (ϵ) are referred to as quasi-energies, and the eigenfunctions of the Floquet Hamiltonian, defined in Eq. (10), are the quasi-energy states. The spectrum of H^F is unbounded; however, we note that in Eq. (7), the eigenvalues (ϵ) of H^F describe the non-periodic evolution of these states as a function of time. Therefore, they are unique modulo Ω, $\epsilon \equiv \epsilon + m\Omega$. The explicit form of the Floquet Hamiltonian for $H(t)$ defined in Eq. (6) is,

$$\begin{aligned} (H^F(\mathbf{k}))_{mn} &\equiv \langle m|H^F(\mathbf{k})|n\rangle, \\ &= (H_0(\mathbf{k}) + n\Omega)\delta_{mn} + \tilde{V}_{mn}, \end{aligned} \tag{11}$$

where,

$$\tilde{V}_{mn} = \frac{1}{T}\int_0^T dt V(t) e^{i(m-n)\Omega t} \tag{12}$$

The integers m and n indexes a particular Floquet block in the matrix H^F. In this representation, the time-independent terms, like H_0, are diagonal, but the time-dependent potential, $V(t)$, acts as a hopping amplitude between various Floquet blocks. These Floquet blocks are like replicas of the original Hamiltonian shifted in quasi-energy by Ω, and the indices will also be referred as the replica index. The quasi-energies can be computed by truncating the matrix after a certain number of Floquet blocks and diagonalizing it.

The Floquet Green function is defined as

$$G^F = \frac{1}{(E\mathbb{1} - H^F)}. \tag{13}$$

All elements of G_F can be rewritten in a closed analytical formula [27] for the special case where the only non-zero components of $\tilde{V}_{mn}$ are $V_- = \tilde{V}_{m+1,m}$ and $V_+ = \tilde{V}_{m,m+1}$ with $m \in \mathbb{Z}$. We mostly restrict ourselves to the $(0,0)$ Floquet block,

$$(G_F)_{00} = \frac{1}{E\mathbb{1} - H_0 - V_{\text{eff}}^+ - V_{\text{eff}}^-}, \tag{14}$$

$$V_{\text{eff}}^{\pm} = V_+ \frac{1}{E \pm \Omega - H_0 - V_+ \frac{1}{E\pm 2\Omega - H_0 - V_+ \frac{1}{\vdots} V_-} V_-} V_-.$$

The Green function can be obtained pertubatively to any order in V by truncating the continued fraction at that order.

FLOQUET TOPOLOGICAL INSULATORS: HALDANE MODEL AND HIGHER CHERN INSULATORS

The topological behavior in the non-equilibrium situation is obtained by choosing a drive of appropriate frequency. We show the non-trivial topology of the quasi-energy bandstructure for the graphene based model in the presence of circularly polarized light.

The tight-binding model on a hexagonal lattice with nearest neighbour hopping and without radiation, in the low energy and linerarized momentum regime reduces to

$$H_0 = v_F(k_x\sigma_z\tau_z + k_y\sigma_y) + M\sigma_z \tag{15}$$

where σ_x and τ_z refer to sublattice isospin and valley degree of freedom respectively, v_F is the fermi velocity at the Dirac points and M is the sublattice mass term. In the presence of circularly polarized light, using Pierels substitution, we have

$$\begin{aligned} H(t) &= v_F((k_x - A_x)\sigma_x\tau_z + (k_y - A_y)\sigma_y) + M\sigma_z \\ \mathbf{A}(t) &= A_0(sin(\Omega t), cos(\Omega t)) \end{aligned} \tag{16}$$

where $\mathbf{A}$ is the vector potential for incident radiation. Consider a general form of the external drive defined in Eq. (6),

$$V(t) = V_+ e^{i\Omega t} + V_- e^{-i\Omega t}, \tag{17}$$

where $V_\pm$ are time-independent operators. Therefore, in the model considered, we have,

$$V_+ = A_0 \left(\frac{i}{2}\sigma_x\tau_z - \frac{1}{2}\sigma_y \right), \quad (18)$$

$$V_- = = V_+^\dagger. \quad (19)$$

Note that the analysis discussed here (see Eq. (15) to Eq. (19)) is valid only in the pertubative low energy regime with $|\mathbf{A}| \ll 1$.

This model breaks time-reversal symmetry, and is classified by the Chern number. We explore two cases, (a) zero resonances, and (b) a single resonance due to radiation and their effects on the topology.

(A) No resonances

This case corresponds to irradiating the system with off-resonant light. The incident frequency of the drive, $\Omega \gg W$, where W is the bandwidth of the time-independent bandstructure. The correction to the energies of the non-equilibrium states are obtained by inspecting the poles of the Floquet Green function. In this case, to lowest order in the radiation potential, the off-diagonal terms in G^F can be ignored. The diagonal element, G^F_{00}, to $O(V^2)$ is,

$$G^F_{00} = \left(E\mathbb{1} - H_0 - \frac{[V_+, V_-]}{\Omega} \right)^{-1} = (E\mathbb{1} - H_{\rm eff})^{-1} \quad (20)$$

where we have a new effective Hamiltonian, $H_{\rm eff}$. Using equations (18), (19) and (20), we note that $H_{\rm eff}$ is equivalent to the Haldane model for anomalous quantum Hall effect with a topological mass $\Delta_0 = \frac{v_F^2 A_0^2}{\Omega}$,

$$H_{\rm eff} = v_F(k_x\sigma_x\tau_z + k_y\sigma_y) + M\sigma_z + \Delta_0\sigma_z\tau_z \quad (21)$$

$$= \begin{pmatrix} \Delta_+ & k_x - ik_y & 0 & 0 \\ k_x + ik_y & -\Delta_+ & 0 & 0 \\ 0 & 0 & \Delta_- & -k_x - ik_y \\ 0 & 0 & -k_x + ik_y & -\Delta_- \end{pmatrix} \quad (22)$$

where τ denotes the valley space, and $\Delta_\pm = M \pm \Delta_0$. The mass gap opens at the Dirac points of the bandstructure near $\epsilon = 0$. The bands will be topological or trivial when $M < \Delta_0$ and $M > \Delta_0$ respectively. Specifically, for $M < \Delta_0$, the Chern number, $C_n = 1$, when measured at quasi-energies in the gap, $-(\Delta_0 - M) < \epsilon < \Delta_0 - M$, and is zero at all other quasi-energies.

(B) Single resonance

This scenario corresponds to the driving frequency in the regime $W/2 < \Omega < W$. The quasi-energy bandstructure has two gaps at (i)$\epsilon = 0$, and (ii) $\epsilon = \pm\Omega/2$, where the topologically non-trivial features may be measured. The gap at $\epsilon = 0$ is the same as that discussed in case (A) and is equal to Δ_0. We incorporate the effect of off-resonant processes on the quasi-energy bandstructure by making the replacement $H_0 \to H_{\rm eff}$ in the Floquet Hamiltonian defined in Eq. (11). For quasi-energies close to resonance, $\epsilon \sim \Omega/2$, adjacent diagonal Floquet blocks, $H_{\rm eff}$, and $H_{\rm eff} - \Omega$, are nearly degenerate. Therefore, to lowest order, H_F must be diagonalized in this subspace of two adjacent Floquet blocks, to obtain the correct quasi-energies. The effective two band Hamiltonian is given by,

$$(H^F)_{\rm eff} = P_\Omega \begin{pmatrix} H_{\rm eff} - \Omega & V_+ \\ V_- & H_{\rm eff} \end{pmatrix} P_\Omega, \quad (23)$$

where P_Ω is the projector onto the bands with quasi-energies in the range $0 < \epsilon < \Omega$. This is exactly the same as degenerate first order perturbation theory, and therefore, the gap exactly at resonance, $\epsilon = \Omega/2$, is proportional to $|V_\pm|$.

The quasi-energies of H^F are periodic in Ω. To properly define a the Chern number for a band (C_n), we must specify its upper and lower bound in quasi-energies. An alternative is to measure the Chern number ($C_n^{\rm trunc}$) of all bands below a particular quasi-energy, for a truncated H^F. It has been shown [15] that this number corresponds to the number of edge states that will be observed at that particular quasi-energy irrespective of chirality. For the case of single resonance, the Chern number of the truncated H^F for $M < \Delta_0$ is

$$C_n^{\rm trun} = \begin{cases} 1 & \text{if } \epsilon = 0 \\ 2 & \text{if } \epsilon = \pm\Omega/2, \end{cases} \quad (24)$$

and for $M > \Delta_0$

$$C_n^{\rm trun} = \begin{cases} 0 & \text{if } \epsilon = 0 \\ 2 & \text{if } \epsilon = \pm\Omega/2, \end{cases} \quad (25)$$

The Chern number of the bands are $C_n = \pm 3$ when $M < \Delta_0$, and $C_n = \pm 2$ when $M > \Delta_0$.

BORN APPROXIMATION: DETAILS

The transition from a trivial state to a topological state is due to renormalization of parameters of the Hamiltonian due to disorder. In the lowest order Born approximation, the correction to the density of states are obtained from exact analytical expressions for the self energy. This provides an accurate description for the density of states as a function of disorder at dilute disorder. The disorder averaged Floquet Green function is given by,

$$\langle G^F(i\omega_n, \mathbf{k}) \rangle = \frac{1}{i\omega_n - H^F(\mathbf{k}) - \Sigma(E)}, \quad (26)$$

and,

$$\Sigma(i\omega_n, \mathbf{k}) = \int_{\rm FBZ} d\mathbf{k}' \ \langle U_{\rm dis}(\mathbf{k}, \mathbf{k}') G^F(i\omega_n, \mathbf{k}') U_{\rm dis}(\mathbf{k}', \mathbf{k}) \rangle, \quad (27)$$

where, $\langle \dots \rangle$ denotes disorder averaging, $U_{\rm dis}(\mathbf{k},\mathbf{k}')$ is the disorder potential in Fourier space, and Σ is the self energy. We are interested at the physics of the topological transition near $\epsilon = 0$ as a function of disorder. For the case of zero resonances, this is correctly modelled by the effective Hamiltonian, $H_{\rm eff}$, defined in Eq. (21). Therefore, instead of using the Floquet Green function, G^F, we use the effective Green function given by,

$$G_0^{\rm eff}(i\omega_n,\mathbf{k}) = \frac{1}{i\omega_n - H_{\rm eff}(\mathbf{k})}. \tag{28}$$

The disorder potential, $U_{\rm dis}$, is modelled as δ-correlated point scatterers. The short range of scattering implies that both inter- and intra-valley processes must be taken into account. It is assumed that, in the linearized regime, the disorder matrix in real space is [28],

$$U_{\rm dis}(\vec{r}) = \sum_i \begin{pmatrix} U_i^A & 0 & U_i^A e^{i\phi_i^A} & 0 \\ 0 & U_i^B & 0 & U_i^B e^{i\phi_i^B} \\ U_i^A e^{-i\phi_i^A} & 0 & U_i^A & 0 \\ 0 & U_i^B e^{-i\phi_i^B} & 0 & U_i^B \end{pmatrix} \tag{29}$$

where,

$$U_i^{A,B} = u_i^{A,B}\delta(\mathbf{r} - \mathbf{r}_i^{A,B}), \tag{30}$$
$$\phi_i^{A,B} = (\mathbf{K}' - \mathbf{K})\cdot \mathbf{r}_i^{A,B}. \tag{31}$$

A and B refer to the different sublattices, $\mathbf{K}$ and $\mathbf{K}'$ are the two valleys, and i is summed over the unit cells. The disorder potentials $u_i^{A,B}$ are taken from an uniform distribution in the range $[-U_0/2, U_0/2]$ and are δ-correlated. Therefore,

$$\langle u_i^A \rangle = \langle u_i^B \rangle = 0, \tag{32}$$
$$\langle u_i^\nu u_j^{\nu'} \rangle = \frac{U_0^2}{12}\delta_{ij}\delta_{\nu\nu'}, \quad \nu,\nu' \equiv A,B, \tag{33}$$

where we have used that the variance of the uniform distribution is $U_0^2/12$. The diagonal and off-diagonal terms in Eq. (29) account for intra- and inter-valley scattering respectively and are assumed to have the same magnitude.

The self energy can be calculated by rewriting $U_{\rm dis}$ (see Eq. (29)) in Fourier space and using Eq. (27) . In the limit of $|\mathbf{k}'| \ll |\mathbf{K} - \mathbf{K}'|$, it can be assumed that, the fast oscillating exponents in the off-diagonal terms in the self energy Eq. (27) averages to zero [28], i.e.,

$$\langle \sum_i e^{i(\mathbf{k}'.r_i^\nu \pm \phi_i^\nu)} \rangle = 0. \tag{34}$$

Therefore, the self energy is diagonal in valley space and independent of momentum $\mathbf{k}$. Consequently, after integrating out the momentum, $\mathbf{k}'$, in the first Brilluoin zone, the four main contribution to the self energy are,

$$\Sigma = \Sigma_I \mathbb{I} + \Sigma_M \sigma_z + \Sigma_\Delta \sigma_z\tau_z + \Sigma_0\tau_z, \tag{35}$$

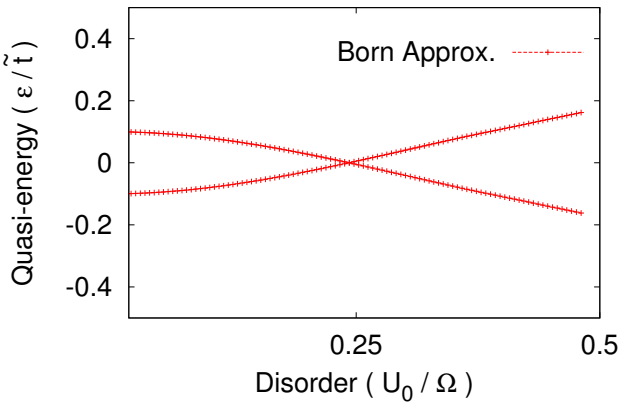

FIG. 5: The expected quasi-energy gap as a function of disorder given by the Born approximation. This is obtained by plotting the solution to the $\tilde{\omega} = \tilde{M} - \tilde{\Delta}_0$ as a function of disorder. The parameters for the system are $A_0 = 1.434$, $\Delta_0 = 0.75$ and $M = 0.85$.

with,

$$\Sigma_I = -nu^2 \frac{i\omega_n}{4\pi v_F^2}\log\left(\frac{v_F^4 D^4}{f_+ f_-}\right), \tag{36}$$
$$\Sigma_M = -\frac{nu^2}{4\pi v_F^2}\left[M\log\left(\frac{v_F^4 D^4}{f_+ f_-}\right) + \Delta\log\left(\frac{f_-}{f_+}\right)\right] \tag{37}$$
$$\Sigma_\Delta = \Sigma_0 = 0, \tag{38}$$

where $f_\pm = \omega_n^2 + (M \pm \Delta_0)^2$. Therefore, the parameters in $H_{\rm eff}(t)$ get renormalized as

$$i\tilde{\omega}_n = i\omega_n - \Sigma_0^I, \tag{39}$$
$$\tilde{M} = M + \Sigma_0^z, \tag{40}$$
$$\text{and,}\quad \tilde{\Delta}_0 = \Delta_0. \tag{41}$$

The renormalized mass, $\tilde{M}$, reduces with increasing disorder. The renormalized quasi-energy is obtained by analytical continuation of $i\omega_n \to \omega$ and the band gap as a function of disorder is the solution to the equation $\tilde{\omega} = \tilde{M} - \tilde{\Delta}_0$. This is shown in Fig. (5) with parameters $v_f = 3/2$, $\Delta = 0.75$ $M = 0.85$ and $D = 4\pi/3$. These parameters correspond to the case (I) of zero resonances. The topological phase transition occurs at the point where the band gap vanishes, which happens when $\tilde{M} = \tilde{\Delta}$. For stronger disorder, the gap reopens in the topological phase and a non-vanishing Chern number must therefore be measured at the quasi- energies in the gap.

BOTT INDEX FOR FLOQUET HAMILTONIAN.

We outline the method to obtain the Chern number of bands for disordered periodically driven Hamiltonians. The Bott index as a measure to obatin the Chern number, was defined by Hastings and Loring [25] for time-independent Hamiltonian. We generalize this formula for periodically driven sys-

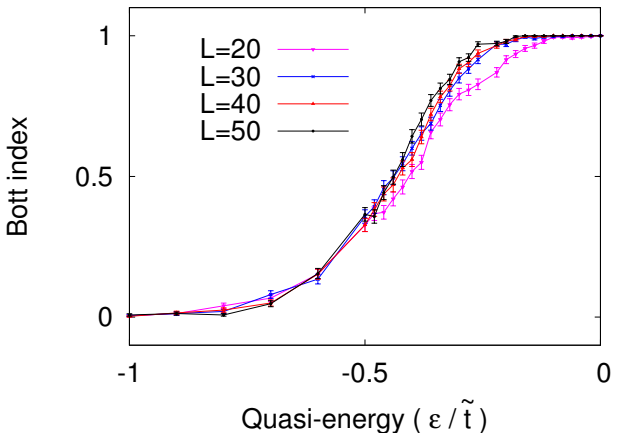

FIG. 6: Finite size effect of the disorder averaged Bott index at disorder strength, $U_0 = 3.5$, for the zero resonance case,as a function of quasi-energy for sizes $L_x = L_y = 20$, 30, 40 and 50. The index has been averaged over 400 disorder realizations.

tems by using the eigenstates of the truncated Floquet Hamiltonian, H^F. This index will measure the number of edge states at a given quasi-energy[15]. Consider a Hamiltonian, $H(t)$ defined on a lattice with periodic boundary conditions (torus geometry). Given two diagonal matrices $X_{ij} = x\delta_{ij}$ and $Y = y\delta_{ij}$ for the x and y coordinates of the lattice sites, let us define two unitary matrices,

$$U_X = \exp(i2\pi X/L_x), \tag{42}$$
$$U_Y = \exp(i2\pi Y/L_y), \tag{43}$$

where $L_{x,y}$ are the dimensions of the system. In the extended Floquet Hilbert space, the analogous definiton for the unitary matrices are,

$$\left(U_X^F\right)_{mn} = U_X\delta_{mn}, \tag{44}$$
$$\left(U_Y^F\right)_{mn} = U_Y\delta_{mn}, \tag{45}$$

where (m, n) refer to a particular Floquet block. For a band of quasi-energies, $\epsilon_l < \epsilon < \epsilon_h$, the Bott index is an integer, and it is well defined as long as the lower and upper bounds, $\epsilon_{l,h}$, are in a mobility gap of the quasi-energy bandstructure. The topological invariant is calculated using the unitary matrices projected onto a band. Let P be the projector onto the chosen band of quasi-energies. In our system, we will be calculating the Bott index of all states with quasi-energies, $\epsilon < 0$, in the truncated Floquet Hamiltonian, H^F. The projected unitary matrices are defined as,

$$\tilde{U}_{X,Y}^F = PU_{X,Y}^F P. \tag{46}$$

For a given disorder configuration, the Bott index of the band is given as,

$$C_b = \frac{1}{2\pi}\mathrm{Im}\left[\mathrm{Tr}\left(\log\left(\tilde{U}_Y^F\tilde{U}_X^F\tilde{U}_Y^{F\dagger}\tilde{U}_X^{F\dagger}\right)\right)\right]. \tag{47}$$

The Bott index is a measure of commutativity of these projected unitary matrices, and it can be shown to be equivalent to the Kubo formula for the Hall conductivity[25]. For a given disorder strength, the Bott index must be averaged over a large number of configurations.

FINITE SIZE EFFECT

We investigate the finite size effect on the non-quantized region of the Bott index when in the Floquet-Anderson topological insulator (FATI) phase.

In Fig. 6, we have plotted the disorder averaged Bott index as a function of quasi-energy for different system sizes. It is clear that with increasing system size, the non-quantized region of the Bott index becomes sharper. This is in agreement with the expectation of a sharp extended state in the bulk quasi-energy band, analogous to a quantum hall state. Therefore, we expect the localization transition to be in the quantum Hall universality class. The current accessible system size is not sufficient to obtain the critical exponents of this transition.